Supplement of Hydrol. Earth Syst. Sci., 27, 3911–3934, 2023
https://doi.org/10.5194/hess-27-3911-2023-supplement
© Author(s) 2023. CC BY 4.0 License.

Hydrology and Earth System Sciences
Open Access

Supplement of

Understanding the compound flood risk along the coast of the contiguous United States

Dongyu Feng et al.

Correspondence to: Zeli Tan (zeli.tan@pnnl.gov)

The copyright of individual parts of the supplement might differ from the article licence.

Supplement

Contents of this file

Tables S1
Figures S1 to S8

Introduction

This supporting material contains a table showing the information of paired USGS gauges and NOAA tidal gauges for uncertainty analysis (Table S1). We also provide ten figures including the MOSART streamflow validation (Fig. S1), GTSM water level validation (Fig. S2), numbers representing individual river basins (Fig. S3) and USGS and NOAA gauges (Fig. S4), and model-data comparison to identify potential CFRA uncertainties at example river basins in Figures S5-S9, and the spatial map of joint exceedance probability ($P_{Q,SS}$) with magnified view at a few representative regions (Fig. S10).

Model-data comparison

We provide a few example basins to demonstrate the various types of uncertainties (Fig. S5-S9). Figures S5~S6 show the epistemic uncertainty caused by inappropriate in-situ locations. In Figure S5, the streamflow measured at the tributary of a mainstem is much lower and cannot represent the river discharge at the outlet. In Figure S6, SS has a different probability distribution than that modeled at the river-ocean interface. Gauge 9419750, despite being close enough to the river outlets, is blocked by man-made barrier islands, thus presenting a different SS signal. Figures S7 show the aleatory uncertainty due to the variability in Q between the USGS gauge and the river outlet. While the probability distributions of Q and SS are similar among the three cases, Q at the upstream gauge typically yields smaller peaks in correspondence to the SS peaks, resulting in lower τ. The epistemic uncertainties in Figures S8~S9 are caused by the GTSM and MOSART models, respectively. In both examples, the dependence between Q and SS is underestimated because GTSM and MOSART underestimate the peaks in SS and Q, respectively. In particular, the MOSART performance is poor in Figure S9, which yields a different Q distribution.

Table S1. Paired USGS and NOAA gauges for uncertainty analysis.

No.	USGS	Latitude and Longitude	NOAA	Latitude and Longitude
1	01034500	45.2361, -68.6514	8413320	44.3922, -68.2043
2	01049265	44.4722, -69.6839	8418150	43.6581, -70.2442
3	01066000	43.8081, -70.7817	8418150	43.6581, -70.2442
4	01113895	41.8884, -71.3814	8452660	41.5050, -71.3267
5	01122500	41.7004, -72.1820	8461490	41.3614, -72.0900
6	01184000	41.9375, -72.6850	8461490	41.3614, -72.0900
7	01389500	40.8847, -74.2261	8518750	40.7006, -74.0142
8	01403060	40.5511, -74.5483	8531680	40.4669, -74.0094
9	01576754	39.9465, -76.3677	8574680	39.2667, -76.5783
10	02037500	37.5632, -77.5469	8638610	36.9467, -76.3300
11	02105769	34.4044, -78.2936	8658120	34.2275, -77.9536
12	02175000	33.0279, -80.3915	8665530	32.7808, -79.9236
13	02198500	32.5286, -81.2683	8670870	32.0367, -80.9017
14	02202500	32.1901, -81.4159	8670870	32.0367, -80.9017
15	02228000	31.1900, -81.9358	8720030	30.6714, -81.4658
16	02246025	30.0825, -81.8094	8720218	30.3982, -81.4279
17	02323592	29.3394, -83.0865	8727520	29.1350, -83.0317
18	02376033	30.6702, -87.2669	8729840	30.4044, -87.2112
19	08068500	30.1105, -95.4363	8771450	29.3100, -94.7933
20	08189500	28.2920, -97.2792	8774770	28.0217, -97.0467
21	11530500	41.4340, -123.9350	9419750	41.7450, -124.1830
22	11532500	41.7915, -124.0762	9419750	41.7450, -124.1830
23	12113000	47.3146, -122.0601	9449880	48.5453, -123.0129
24	12150800	47.8309, -122.0485	9449880	48.5453, -123.0129
25	12213100	48.8448, -122.5893	9449880	48.5453, -123.0129
26	14243000	46.2748, -122.9146	9439040	46.2073, -123.7683

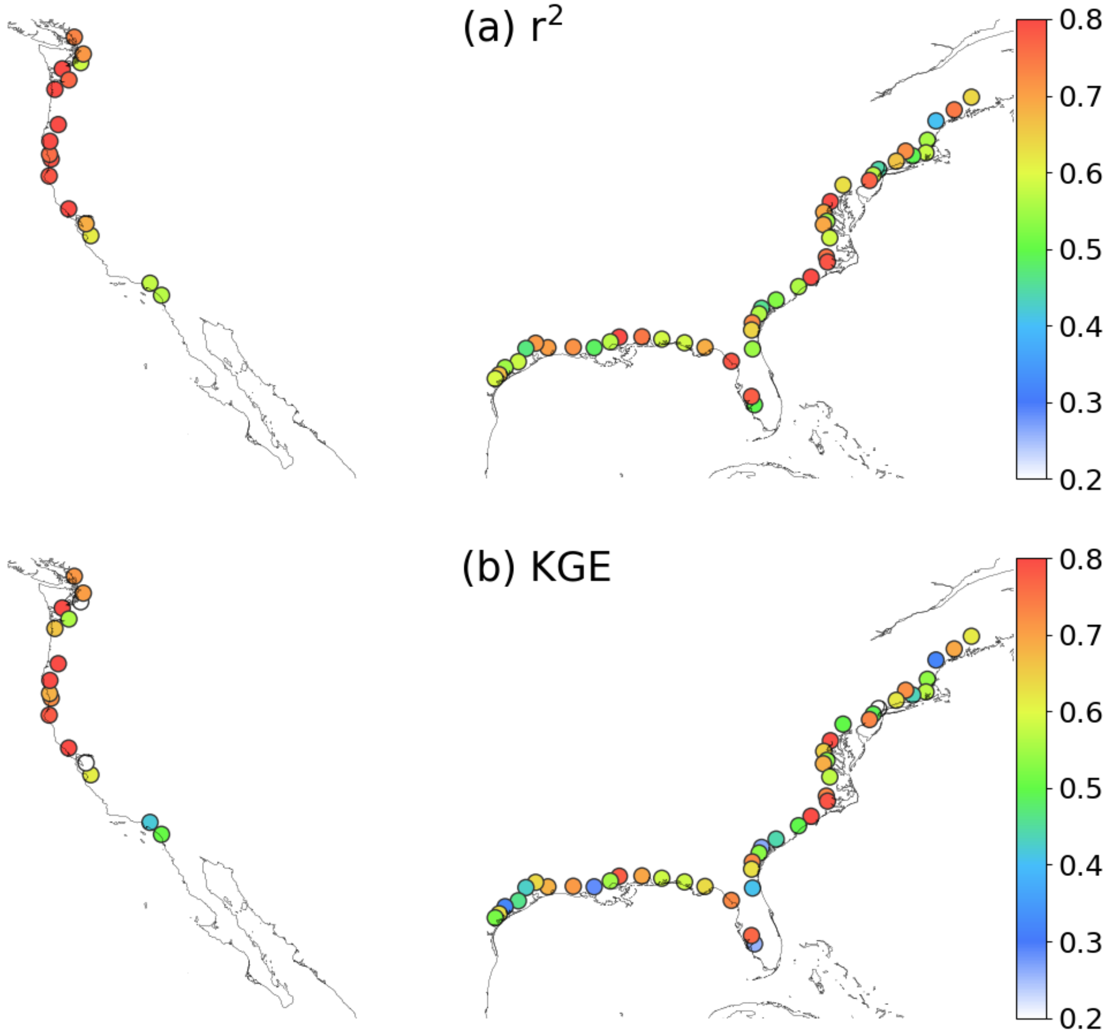

Figure S1. The evaluation of the MOSART simulated streamflow at the selected USGS gauges near the CONUS coastline using: (a) coefficient of determination r^2; (b) Kling-Gupta efficiency (KGE) (Gupta et al., 2009).

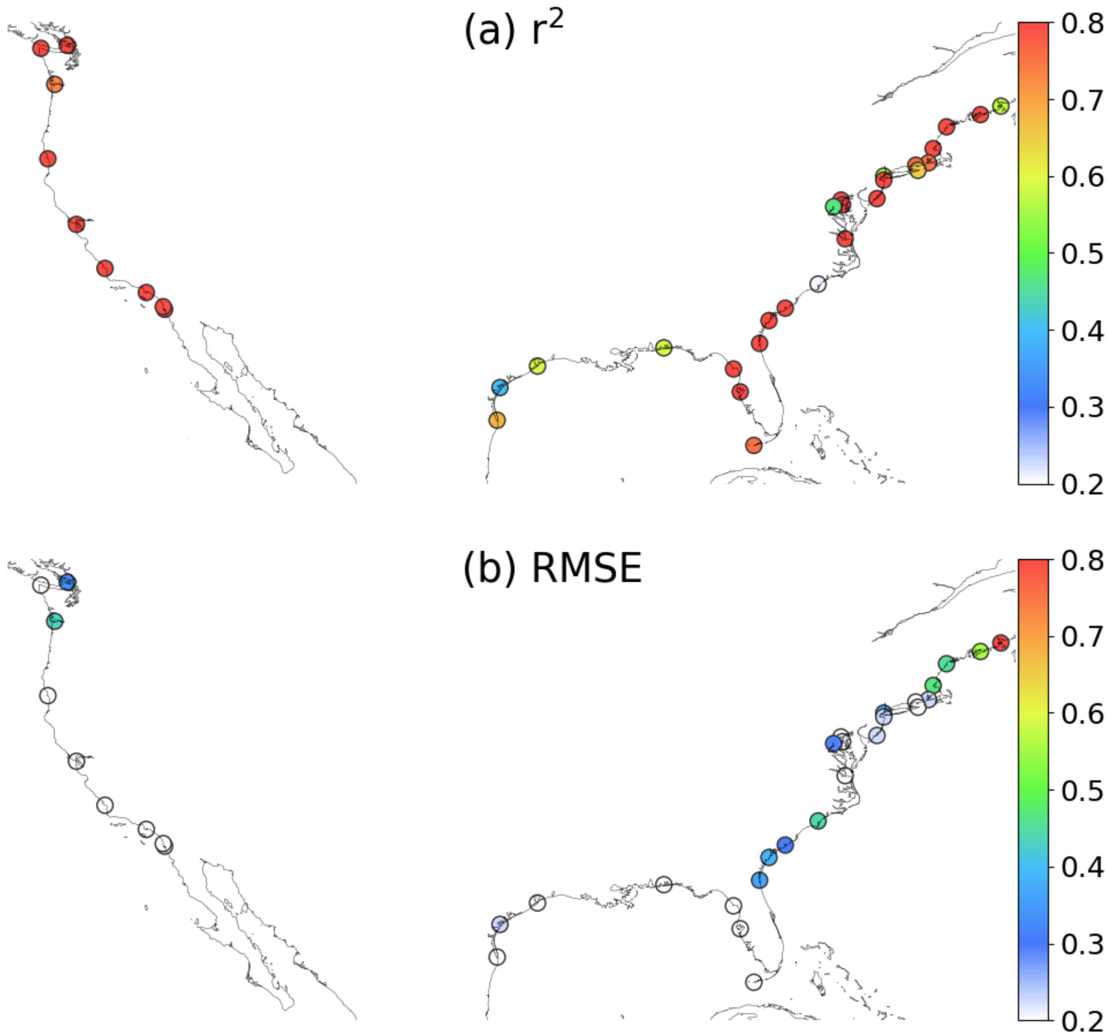

Figure S2. The evaluation of the GTSM modeled total water level at the selected NOAA tidal gauges near the US coastline using: (a) coefficient of determination r^2; (b) root mean squared error (RMSE).

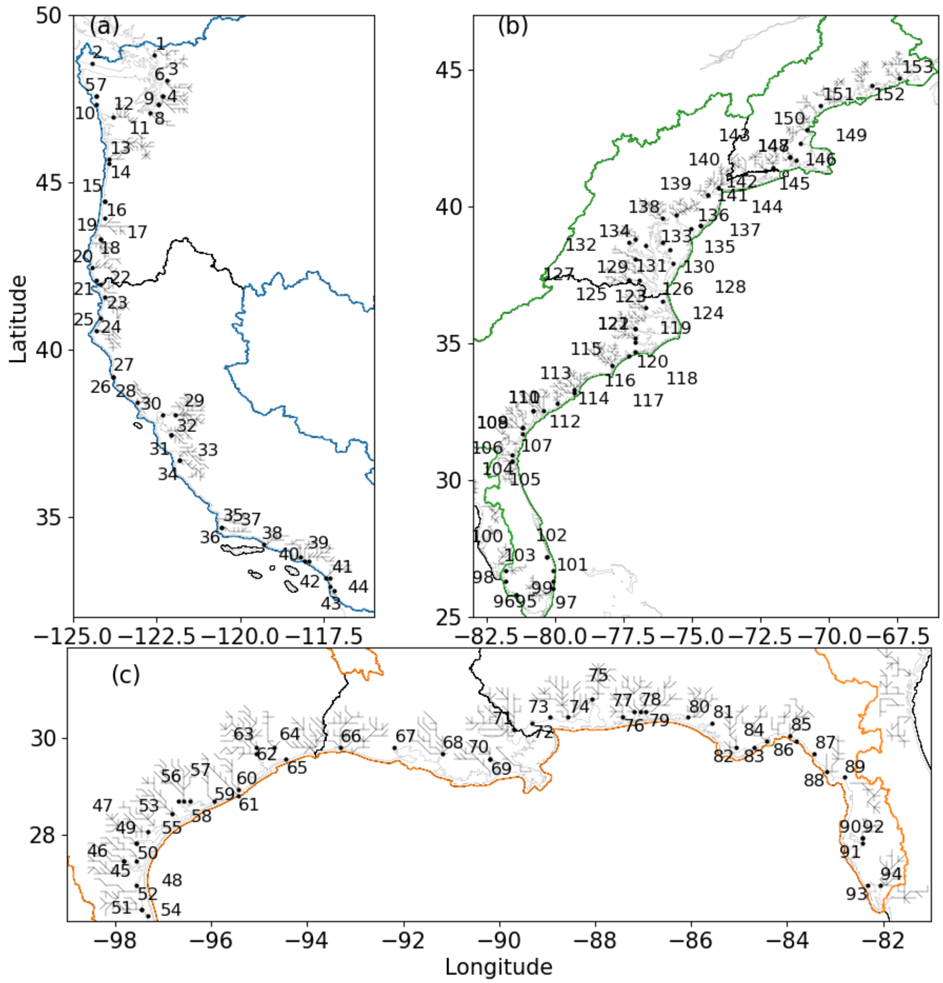

Figure S3. The numbers representing individual river basins corresponding to those in Figure 4.

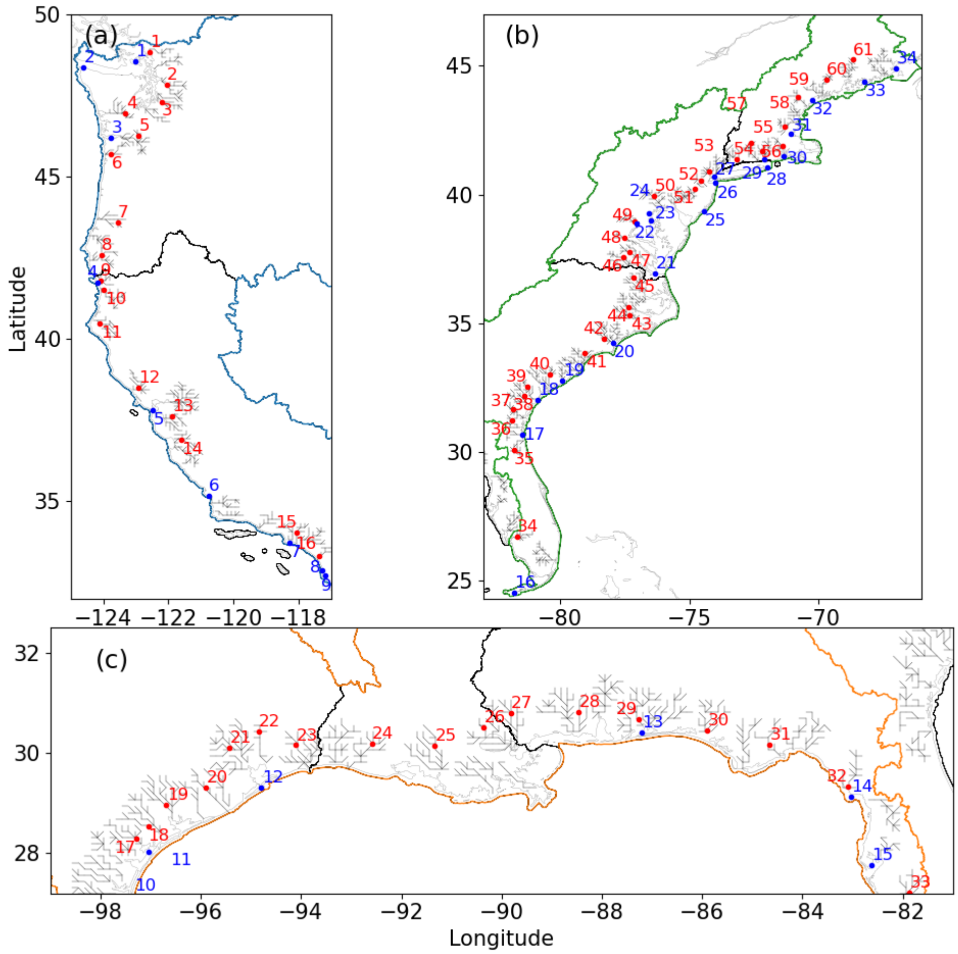

Figure S4. The numbers representing USGS gauges (red) and NOAA gauges (blue) corresponding to those in Figure 6.

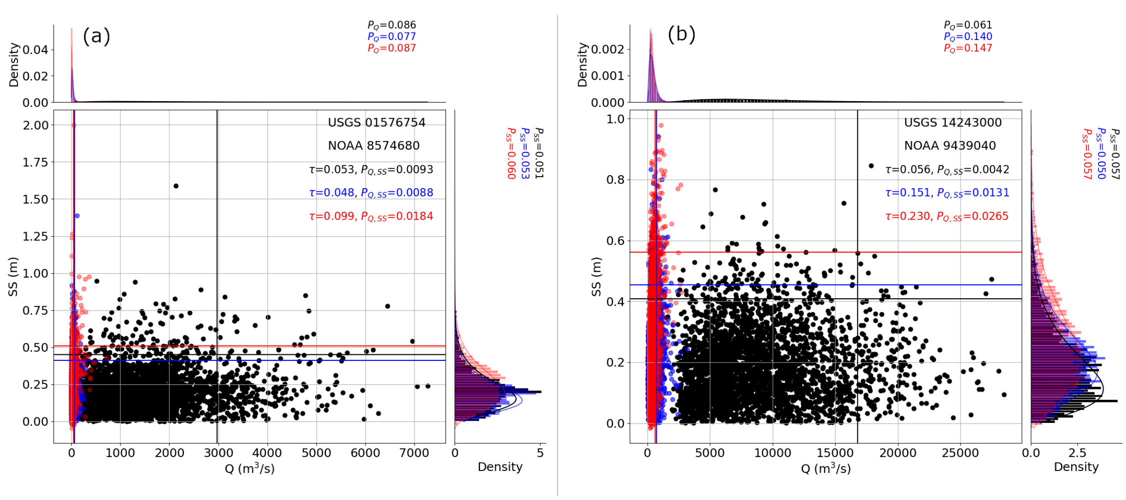

Figure S5. Epistemic uncertainty caused by the inappropriate USGS gauge locations. The uncertainty is identified by model-data comparison at the river basins corresponding to USGS gauge 01576754 and 14243000.

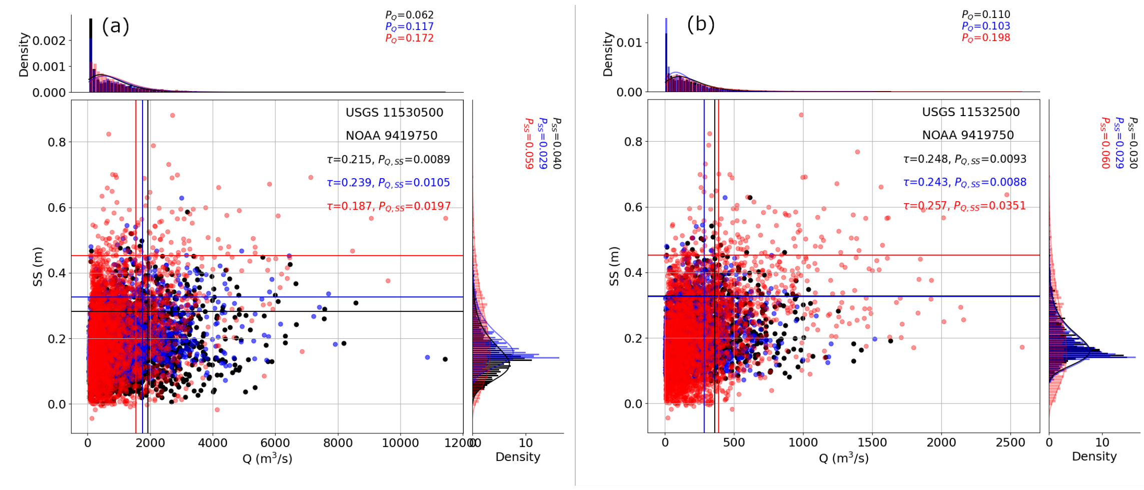

Figure S6. Epistemic uncertainty caused by the inappropriate NOAA gauge locations. The uncertainty is identified by model-data comparison at the river basins corresponding to USGS gauge 11530500 and 11532500.

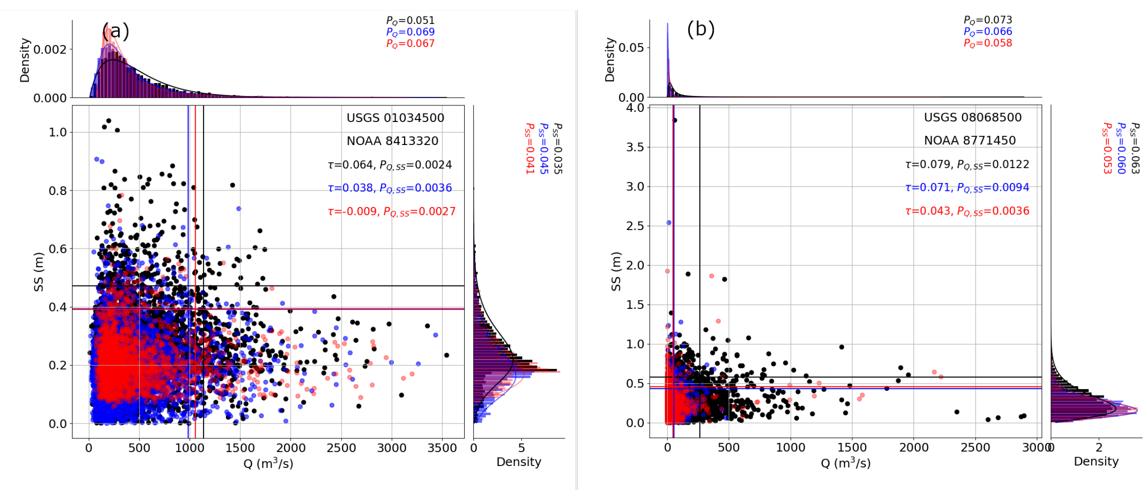

Figure S7. Aleatory uncertainty due to the variability in Q. The uncertainty is identified by model-data comparison at the river basins corresponding to USGS gauge 01034500 and 08068500.

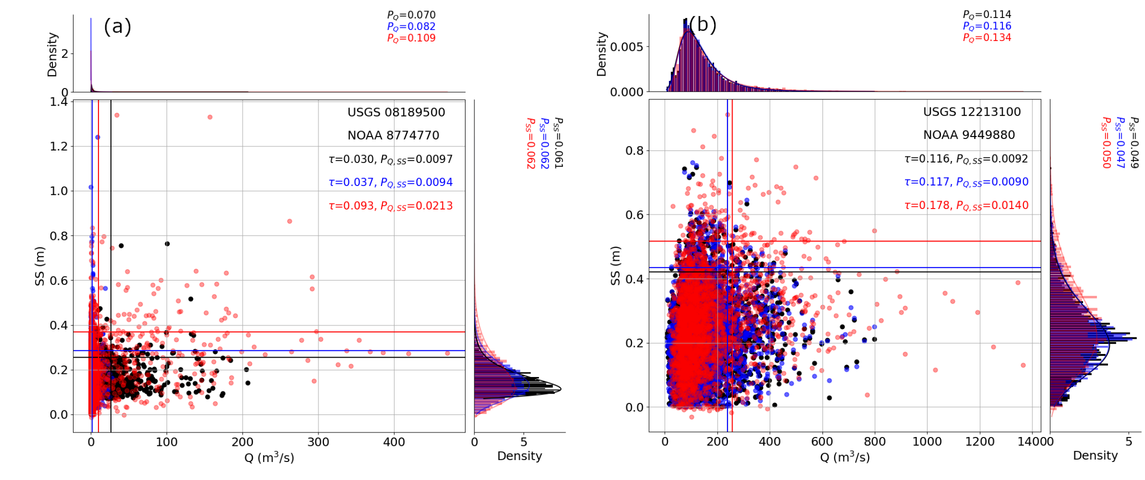

Figure S8. Epistemic uncertainty due to the underestimation of *SS* peaks in GTSM. The uncertainty is identified by model-data comparison at the river basins corresponding to USGS gauge 08189500 and 12213100.

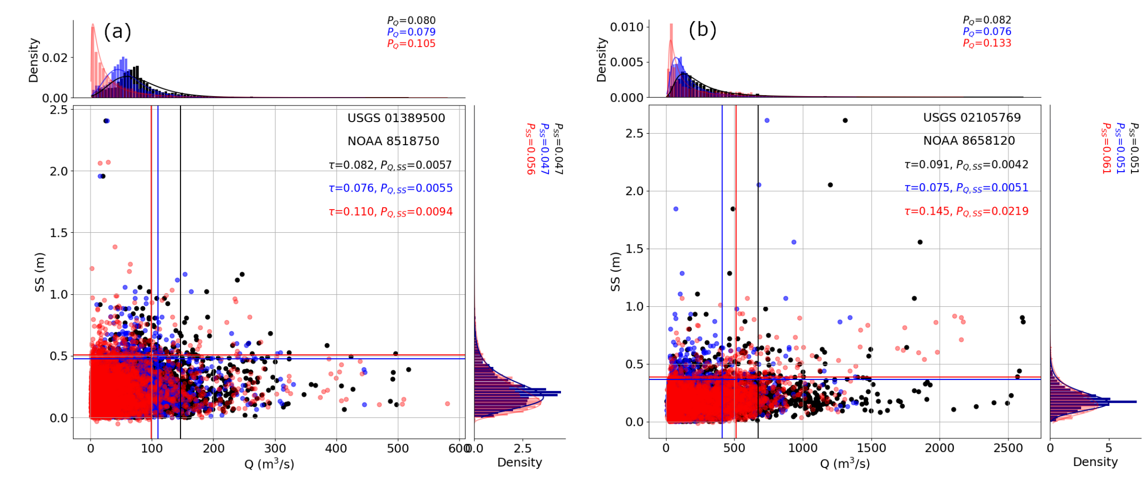

Figure S9. Epistemic uncertainty due to the reduced MOSART performance. The uncertainty is identified by model-data comparison at the river basins corresponding to USGS gauge 01389500 and 02105709.

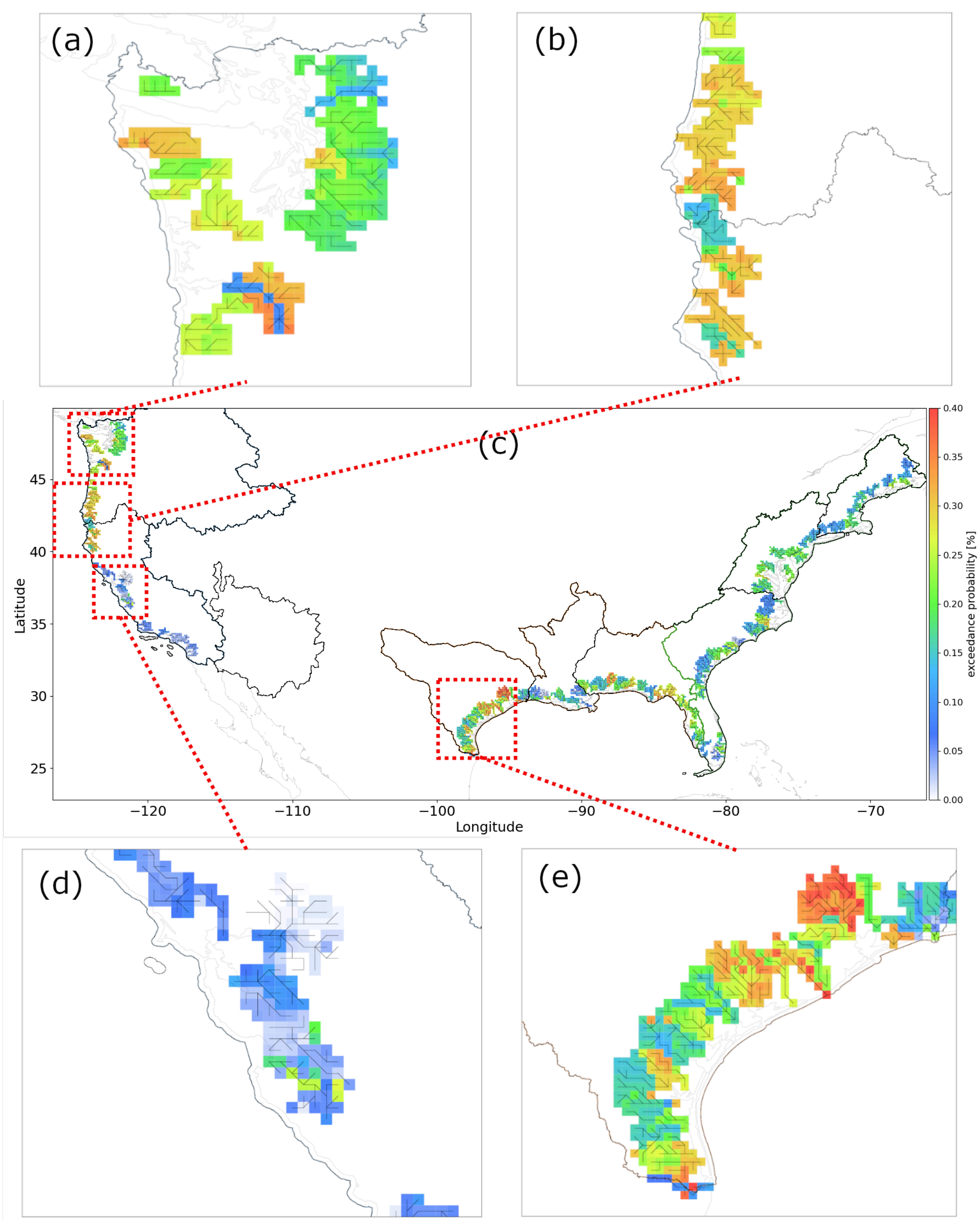

Figure S10. The joint exceedance probability ($P_{Q,SS}$) in CONUS with magnified views at four representative regions where $P_{Q,SS}$ is significantly different in the mainstem than its tributaries.

References

Gupta, H. V., Kling, H., Yilmaz, K. K., and Martinez, G. F.: Decomposition of the mean squared error and NSE performance criteria: Implications for improving hydrological modelling, Journal of hydrology, 377, 80-91, 10.1016/j.jhydrol.2009.08.003, 2009.